Extensions to Dynamically-Consistent Collision Reaction Control for Collaborative Robots

Harder, Marie and Iskandar, Maged and Lee, Jinoh and Dietrich, Alexander


```
@Article{harder2023extensions,
  author    = {Harder, Marie and Iskandar, Maged and Lee, Jinoh and Dietrich, Alexander},
  journal   = {2023 IEEE/RSJ International Conference on Intelligent Robots and Systems (IROS)},
  title     = {Extensions to Dynamically-Consistent Collision Reaction Control for Collaborative Robots},
  year      = {2023},
  publisher = {IEEE},
}
@Comment{jabref-meta: databaseType:bibtex;}
```

Extensions to Dynamically-Consistent Collision Reaction Control for Collaborative Robots

Marie Harder[1], Maged Iskandar[1], Jinoh Lee[1,2] and Alexander Dietrich[1]

Abstract— **Since modern robots are supposed to work closely together with humans, physical human-robot interaction is gaining importance. One crucial aspect for safe collaboration is a robust collision reaction strategy that is triggered after an unintentional physical contact. In this work, we propose a dynamically-consistent collision reaction controller, where the reactive motion is performed in one particular desired direction in Cartesian space, without disturbing the remaining ones. This results in more intuitive and more predictable behavior of the end-effector. In addition, the proposed reaction control law is independent of contact and internal observer dynamics used for collision detection. The theoretical claims are validated in simulation and experiments. The proposed reaction controller is experimentally compared with a conventional approach for collision reaction. All experiments have been conducted on a torque controlled KUKA LWR IV+ lightweight robot.**

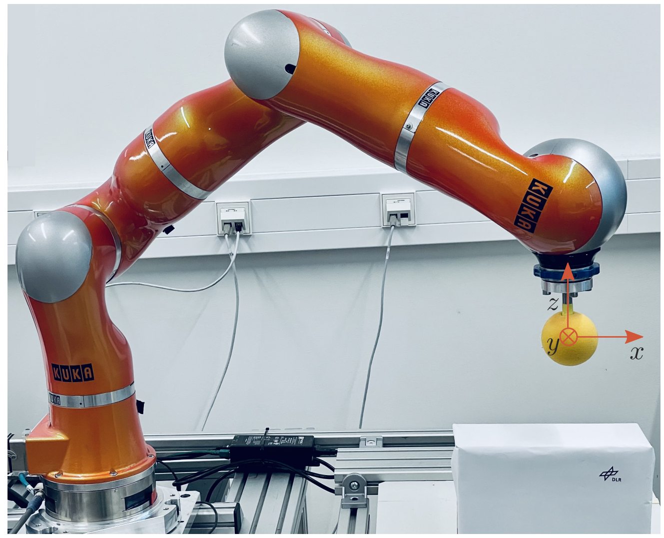

Fig. 1. The torque controlled KUKA LWR IV+ robot with 7 DoF is used for experimental evaluation of the collision reaction strategies.

I. Introduction

As today's robots are supposed to work closely with humans, safe physical human-robot interaction (pHRI) has become an important field of research. Undesired collisions between the robot and humans should be prevented and unavoidable physical contacts should be handled in a safe and predictable way. An extensive overview of the different phases of robot collision handling is given in [1]. In the pre-collision phase the aim is to completely avoid undesired physical contacts. Therefore one can either define forbidden areas in the workspace of the robot [2] or use information from external sensors such as on-board vision [3] or proximity sensors [4].

During the impact phase, the use of lightweight robots [5], compliant joints [6], or protective soft covering [7], [8] can help to reduce the impact force by design. A protective soft skin as presented in [8] can not only be used as passive padding. If it is additionally equipped with sensors, it can provide valuable information for collision detection and localization. There are many other techniques for collision detection that only rely on proprioceptive sensor information and are therefore very attractive [9], [7]. A popular method is the momentum-based observer for collision detection [16] and its various extensions such as [11]. It has the advantage that no joint acceleration or inversion of the inertia matrix is needed.

This work was supported by ITECH R&D programs of MOTIE/KEIT under Grants 20014398 and 20014485.

[1]The authors are with the Institute of Robotics and Mechatronics, German Aerospace Center (DLR), Münchner Str. 20, 82234 Weßling, Germany marie.harder@dlr.de

[2]The author is also with the Department of Mechanical Engineering, Korea Advanced Institute of Science and Technology (KAIST), 34141 Daejeon, Republic of Korea.

After a collision has been detected, a collision reaction strategy should be triggered, in order to reduce the impact of the collision and thus prevent the human operator and the robot from being harmed. The most trivial strategy is to stop the robot immediately after detecting the collision either by engaging the brakes or by switching to a high-gain position controller with the desired link position being the one at the moment of collision detection [12], [13], [14]. Stopping the robot can lead to situations, where parts of the body of the human operator are clamped. For safer human-robot interaction, the preferred alternative is to switch to zero-gravity control mode after the collision occurred [15]. That enables the operator to freely move the manipulator away from the critical configuration and push it away from the point of collision. Numerous methods for collision detection provide additional information on the collision to be exploited in the reaction control [11], [16]. For example the momentum-based observer [10] yields a residual whose directional information can be used in order to bounce back from the collision along the same resulting direction [16]. This approach is well-established as *reflex strategy* and widely deployed in real world applications [17], [18].

In all of the collision reaction strategies mentioned so far, the current motion path is aborted. In contrast to that, in [19] the desired motion path is preserved, even if a collision occurred. Through scaling of the trajectory in time, it is possible to step back and forth along the desired motion path

[19]. If a collision is detected, the robot moves back along the trajectory. Thus, a compliant behavior is achieved, while the original motion path is preserved. Another approach that preserves the original task as best as possible was proposed in [18] and makes use of kinematic redundancy. Unlike most of the reaction controllers, which are operating on joint-level, [18] exploits the task-space. The main objective is to follow a Cartesian reference trajectory of the end-effector with a robot that is kinematically redundant with respect to the main task. Using a dynamically consistent null space projector, the reflex torque [19] is included in the null space of the original task in order to not affect task execution [18]. If that is not sufficient and the impact force still exceeds a defined threshold, the original task can be partially relaxed [18].

Inspired by the exploitation of kinematic redundancy during collision reaction [18], we propose an alternative method of dynamically-consistent collision reaction control. To comply with the solution of nature, the "acceleration energy" [20] should be minimized. That optimization leads to an interpretation of the dynamically-consistent null space projector [21]. In contrast to [18], in this paper the collision reaction control is not projected onto the null space of a main task, but onto the null space of directions, in which no accelerations should occur. The contribution of the paper is the development of a collision reaction controller that results in a reactive motion in only one particular direction. This makes the behavior of the end-effector more predictable and can be useful in applications, where the manipulator operates in proximity to delicate surfaces, that should not be damaged. Furthermore the proposed strategy is not dependent on observer dynamics. The theoretical findings are evaluated in simulation and in experiments on a torque controlled KUKA LWR IV+ lightweight robot.

After some preliminaries in Sec. II, the derivation of the dynamically-consistent collision reaction control is introduced in Sec. III. Results from simulation are shown in Sec. IV. Sec. V presents the experiments and a conclusion is drawn in Sec. VI.

II. Preliminaries

The rigid-body dynamics of a manipulator with n degrees of freedom (DoF) can be written as

$$\boldsymbol{M}(\boldsymbol{q})\ddot{\boldsymbol{q}} + \boldsymbol{C}(\boldsymbol{q}, \dot{\boldsymbol{q}})\dot{\boldsymbol{q}} + \boldsymbol{g}(\boldsymbol{q}) = \boldsymbol{\tau} + \boldsymbol{\tau}_{\text{ext}} \quad (1)$$

with $\boldsymbol{q}, \dot{\boldsymbol{q}}, \ddot{\boldsymbol{q}} \in \mathbb{R}^n$ being the link-side positions, velocities, and accelerations, respectively. The symmetric and positive definite inertia matrix is denoted by $\boldsymbol{M}(\boldsymbol{q}) \in \mathbb{R}^{n\times n}$, and the generalized gravity forces are represented by $\boldsymbol{g}(\boldsymbol{q}) \in \mathbb{R}^n$. The Coriolis and centrifugal matrix $\boldsymbol{C}(\boldsymbol{q}, \dot{\boldsymbol{q}}) \in \mathbb{R}^{n\times n}$ is formulated such that $\dot{\boldsymbol{M}}(\boldsymbol{q}, \dot{\boldsymbol{q}}) = \boldsymbol{C}(\boldsymbol{q}, \dot{\boldsymbol{q}}) + \boldsymbol{C}(\boldsymbol{q}, \dot{\boldsymbol{q}})^T$ holds [22]. The quantities $\boldsymbol{\tau}, \boldsymbol{\tau}_{\text{ext}} \in \mathbb{R}^n$ describe the control inputs and generalized external forces, respectively.

The generalized external forces $\boldsymbol{\tau}_{\text{ext}}$ can be estimated using a momentum-based observer [16]. Using the generalized momentum $\boldsymbol{p} = \boldsymbol{M}(\boldsymbol{q})\dot{\boldsymbol{q}}$ as monitoring signal, a residual vector $\boldsymbol{r}$ [16] can be defined as

$$\boldsymbol{r}(t) = \boldsymbol{K}_o \left(\boldsymbol{p}(t) - \int_0^t (\boldsymbol{\tau} - \boldsymbol{n}(\boldsymbol{q}, \dot{\boldsymbol{q}}) + \boldsymbol{r}) dt - \boldsymbol{p}(0) \right) \quad (2)$$

The diagonal matrix of observer gains is denoted by $\boldsymbol{K}_o > \boldsymbol{0}$. For a more compact presentation, the term $\boldsymbol{n}(\boldsymbol{q}, \dot{\boldsymbol{q}}) = \boldsymbol{g}(\boldsymbol{q}) - \boldsymbol{C}(\boldsymbol{q}, \dot{\boldsymbol{q}})^T\dot{\boldsymbol{q}}$ is introduced. From the dynamics of the residual results $\boldsymbol{r} \approx \boldsymbol{\tau}_{\text{ext}}$ for the limit case $\boldsymbol{K}_o \to \infty$ [16]. One can specify a limit $\boldsymbol{\tau}_{\text{limit}} \in \mathbb{R}^n$ for the joint torques, with $r_{\text{limit},j}$ $(j = 1, ..., n)$ being the components of $\boldsymbol{\tau}_{\text{limit}}$. If the condition $|r_j| > r_{\text{limit},j}$ with $j = 1, ..., n$ is satisfied, a collision will be detected.

III. Dynamically-Consistent Collision Reaction Control

In this paper, a dynamically-consistent collision reaction controller is proposed, where the reactive motion of the end-effector of the robot after a collision is performed in one particular direction in Cartesian space. It is assumed that this direction is known. In practice it can be obtained from a vision system or tactile sensors.

The basic idea of the proposed collision reaction strategy is to minimize, what was introduced in [20] as "acceleration energy" which is the solution of nature that complies with the Gauss- and D'Alembert principles [21]. This quantity is to be minimized under the constraint that there is no acceleration in all directions that are not the specified direction for the reactive motion. That can be formulated as quadratic optimization

$$\begin{aligned} &\min_{\boldsymbol{\tau}} \frac{1}{2}\tilde{\boldsymbol{\tau}}^T \boldsymbol{M}(\boldsymbol{q})^{-1}\tilde{\boldsymbol{\tau}} \\ &\boldsymbol{J}_R(\boldsymbol{q})\boldsymbol{M}(\boldsymbol{q})^{-1}\boldsymbol{\tau} = \boldsymbol{0}, \end{aligned} \quad (3)$$

with $\tilde{\boldsymbol{\tau}} = \boldsymbol{\tau} - \boldsymbol{\tau}_0$. The Jacobian $\boldsymbol{J}(\boldsymbol{q}) \in \mathbb{R}^{6\times n}$ of the end-effector of the robot is separated into $\boldsymbol{J}_c(\boldsymbol{q}) \in \mathbb{R}^{1\times n}$, which describes the direction of the desired reactive motion and $\boldsymbol{J}_R(\boldsymbol{q}) \in \mathbb{R}^{5\times n}$ being the remaining rows of $\boldsymbol{J}(\boldsymbol{q})$. The torque $\boldsymbol{\tau}_0$ is defined as $\boldsymbol{\tau}_0 = \boldsymbol{J}_c(\boldsymbol{q})^T F_{\text{des}}$ with $F_{\text{des}} = \Omega_c a_{\text{des}}$. Herein a_{des} denotes the desired acceleration that pushes away from the collision. The respective collision inertia is described by Ω_c:

$$\Omega_c = (\boldsymbol{J}_c(\boldsymbol{q})\boldsymbol{M}(\boldsymbol{q})^{-1}\boldsymbol{J}_c(\boldsymbol{q})^T)^{-1}. \quad (4)$$

The desired acceleration a_{des} together with the collision inertia Ω_c leads to the force F_{des} pushing away from the collision. In case the desired direction for the reactive motion does not align with one Cartesian direction of the end-effector, one can use a transformation to change the frame of reference of the Jacobian $\boldsymbol{J}(\boldsymbol{q})$.

To solve the optimization problem (3), one can use the standard method of Lagrange multipliers [23]. The corresponding Lagrangian function is

$$\mathcal{L}(\boldsymbol{\tau}, \boldsymbol{\lambda}) = \frac{1}{2}\tilde{\boldsymbol{\tau}}^T \boldsymbol{M}(\boldsymbol{q})^{-1}\tilde{\boldsymbol{\tau}} + \left[\boldsymbol{J}_R(\boldsymbol{q})\boldsymbol{M}(\boldsymbol{q})^{-1}\boldsymbol{\tau}\right]^T \boldsymbol{\lambda} \quad (5)$$

with $\boldsymbol{\lambda} \in \mathbb{R}^5$ being the Lagrange multiplier. Solving that, yields

$$\boldsymbol{\tau} = \boldsymbol{N}_{\text{dyn}}(\boldsymbol{q})\boldsymbol{J}_c(\boldsymbol{q})^T \Omega_c a_{\text{des}} \quad (6)$$

with

$$\boldsymbol{N}_{\text{dyn}}(\boldsymbol{q}) = \boldsymbol{I} - \boldsymbol{J}_R(\boldsymbol{q})^T \boldsymbol{\Omega}_R \boldsymbol{J}_R(\boldsymbol{q}) \boldsymbol{M}(\boldsymbol{q})^{-1} \tag{7}$$

$$\boldsymbol{\Omega}_R = (\boldsymbol{J}_R(\boldsymbol{q}) \boldsymbol{M}(\boldsymbol{q})^{-1} \boldsymbol{J}_R(\boldsymbol{q})^T)^{-1}. \tag{8}$$

With that reaction control law (6) one can apply a desired acceleration a_{des} away from the collision, which together with Ω_c defines the respective force F_{des} in the direction of the reactive motion. With $\boldsymbol{J}_c(\boldsymbol{q})^T$ this Cartesian force is mapped back to joint space and the dynamically-consistent null space projector $\boldsymbol{N}_{\text{dyn}}(\boldsymbol{q})$ [21] projects the joint torques onto the null space of $\boldsymbol{J}_R(\boldsymbol{q})$. Meaning that the generated torques will lead to zero accelerations in the undesired directions.

To avoid unlimited reactive motion after a collision, one possible approach is to design the scalar desired acceleration a_{des} in such a way that it has its maximum value at the beginning ($a_{\text{des},0}$) and then goes to zero after the end-effector moved away a defined distance. Since it is desirable to have the strongest reaction at the beginning, it is reasonable to have the maximum value of a_{des} at the beginning and even scale it to the maximum torques of the individual axes.

IV. Validation in Simulation

For the validation of the theoretical claims made in Sec. III, we simulate a 7-DoF robotic manipulator in MATLAB Simulink. The initial configuration of the end-effector of the robot is $\boldsymbol{q}_0 = \left[-0.44, 0.9, 0.68, -1.1, 0.2, -0.4, 1.6\right]^T$ rad, where the robot is at rest. A PD+ joint controller [24] holds the robot at $\boldsymbol{q}_0$ until the collision reaction strategy is triggered automatically at a fixed time $t = 0.1\,\text{s}$. The direction specified for the reactive motion is the Cartesian x-direction at the end-effector (see Fig. 1).

In simulation the proposed reaction control (6) is compared with one omitting the projection:

$$\boldsymbol{\tau}_{\text{compare}} = \boldsymbol{J}_c(\boldsymbol{q})^T \Omega_c a_{\text{des}}. \tag{9}$$

Except for the pre-multiplication by the dynamically-consistent null space projector in (6), both are equivalent.

To provide the conditions for a fair comparison, the initial desired acceleration $\ddot{x}_{\text{des},0}$ in both methods are chosen such that the peak acceleration in the reaction direction is similar. This can be seen in the upper plot of Fig. 2. At time $t = 0.1\,\text{s}$, when the collision reaction strategy is activated, the peak accelerations for both strategies match.

The upper three plots of Fig. 2 show the acceleration of the end-effector in x-,y-,z-directions and the three plots below the angular acceleration in terms of the Euler angles $\ddot{\phi}_x, \ddot{\phi}_y$ and $\ddot{\phi}_z$. Following the theory from Sec. III one would only expect an acceleration in x-direction for the proposed reaction control with null space projector (6). The accelerations in the remaining directions should be zero. This is also illustrated in Fig. 2, showing the results from the simulation. With the proposed reaction controller (6) there is only a sudden change in acceleration in the desired x-direction and only small drift in the other directions (dashed line in Fig. 2). In contrast to that we see accelerations in all six Cartesian directions with the approach without null space projector (9) (solid line in Fig. 2).

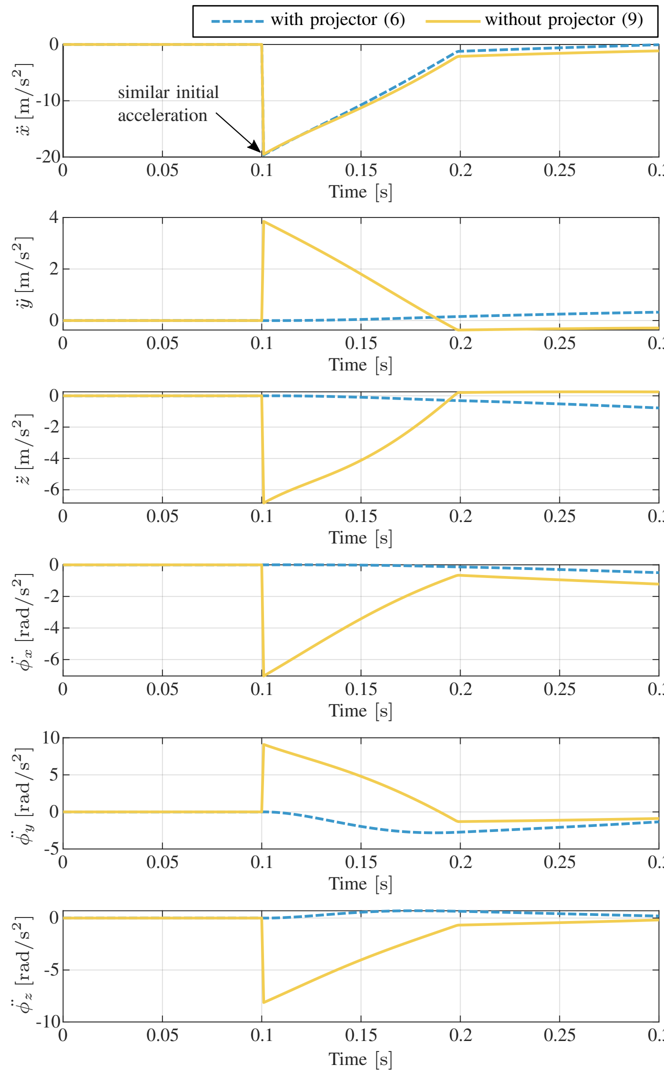

Fig. 2. Acceleration of the end-effector in x-,y-,z-directions (upper three plots) and angular acceleration in terms of the Euler angles $\ddot{\phi}_x, \ddot{\phi}_y, \ddot{\phi}_z$ (lower three plots) with the proposed strategy with dynamically-consistent null space projector (6) (dashed) and the method without projection (9) (solid) in simulation.

How the position of the end-effector of the robot evolves under the two different collision reaction strategies can be observed in Fig. 3. During the time period shown in Fig. 3 the end-effector moves almost $0.2\,\text{m}$ in the desired x-direction. With the proposed control law (6) the motion in y- and z-directions is only about $2\,\text{mm}$ and $4\,\text{mm}$, respectively (dashed line in Fig. 3). This slight deviation in position is mainly due to small numerical drift in the acceleration signal and the fact that it is integrated twice through the robot dynamics. With the strategy without projection (9) the deviation is about $28\,\text{mm}$ in y-direction and $60\,\text{mm}$ in z (solid line in Fig. 3).

The results from the simulation show that with the proposed controller (6) we can limit the reactive motion to

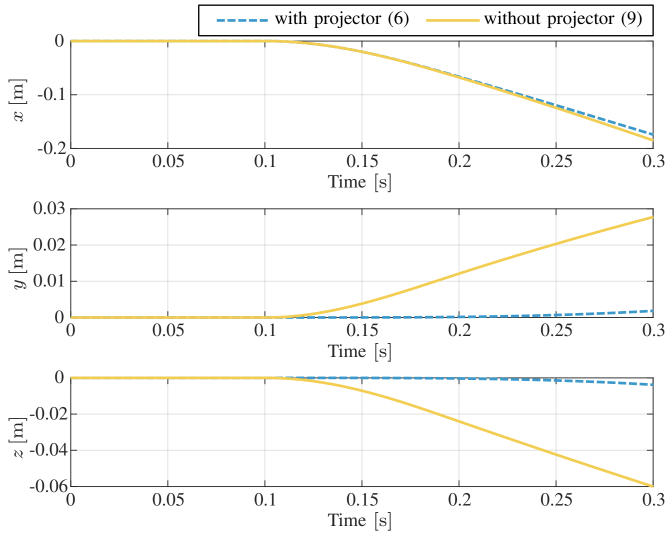

Fig. 3. Position of the end-effector in x-,y-,z-directions with the proposed strategy with dynamically-consistent null space projector (6) (dashed) and the method without projection (9) (solid) in simulation.

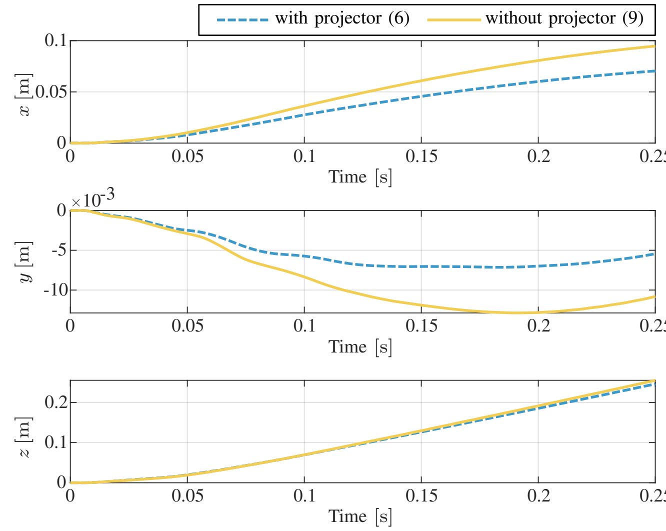

Fig. 5. Experiment 1: Position of the end-effector in x-,y-,z-directions with the proposed strategy with dynamically-consistent null space projector (6) (dashed) and the method without projection (9) (solid)

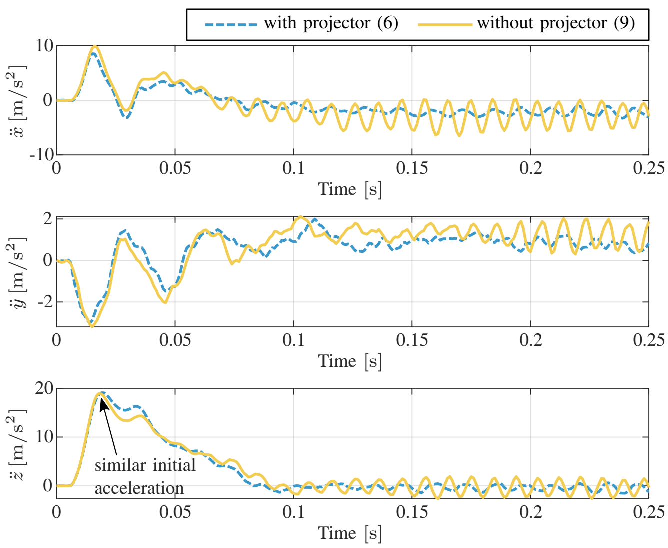

Fig. 4. Experiment 1: Acceleration of the end-effector in x-,y-,z-directions with the proposed strategy with dynamically-consistent null space projector (6) (dashed) and the method without projection (9) (solid)

one particular direction in Cartesian space. The theoretical claims made in Sec. III hold in simulation. In the following, experiments are made on real hardware for which, in contrast to the simulation, there is no perfect model available.

V. Experimental Evaluation

The experiments are conducted on a KUKA LWR IV+ robot with seven DoF as shown in Fig. 1. The robot starts at the initial configuration $\boldsymbol{q}_0 = \left[-0.2, 0.9, -0.21, -1.1, 0.20, 1.14, 0\right]^T$ rad . For all experiments on the hardware z is the direction of the desired reactive motion (Fig. 1).

In the first experiment the robot is initially at rest until the collision reaction strategy is manually triggered. We scale the desired acceleration profile such that the peak-accelerations $\ddot{z}_{\max}$ of both reaction strategies are similar (see Fig. 4). That results in an initial desired acceleration $\ddot{z}_{\mathrm{des},0} = 30\,\mathrm{m/s^2}$ for the proposed strategy (6) and $\ddot{z}_{\mathrm{des},0} = 25.8\,\mathrm{m/s^2}$ for the method without projection (9). Looking at the accelerations in x- and y-directions (Fig. 4) the difference between the two reaction strategies is not as visible as in simulation (Sec. IV, Fig. 2). Although with the proposed control (6) we aimed at only accelerating in one predefined direction, the experiments on the real hardware show that the end-effector is also accelerated in the other directions. This can be due to errors in the inertial model or unmodeled friction. The effect of friction could be reduced by using model-based friction compensation techniques [25], [26] and/or motor disturbance observers [27]. Noticeably, even the small amplitude oscillations in the acceleration signal during motion are dynamically coupled in the reaction control without projection (9) (solid line in Fig. 4).

The visualization of the position of the end-effector in x-, y- and z-directions, shown in Fig. 5, reflects the same behavior. While the end-effector moves about $0.25\,\mathrm{m}$ in the desired z-direction, the deviation in x-direction is $0.07\,\mathrm{m}$ and $0.095\,\mathrm{m}$ and in y-direction $0.005\,\mathrm{m}$ and $0.011\,\mathrm{m}$ for the proposed strategy (6) and the method without dynamically-consistent null space projector (9), respectively. One can still see a smaller deviation in the remaining directions, when using the projection, but the difference is not as significant as in the simulation (Sec. IV).

In the second experiment the proposed collision reaction controller is compared to a well-known reaction strategy, called the reflex strategy [16]:

$$\boldsymbol{\tau}_{\text{reflex}} = \boldsymbol{K}_{\text{reflex}}\boldsymbol{r}. \tag{10}$$

The vector $\boldsymbol{r} \in \mathbb{R}^n$ (2) describes the residual from the momentum-based observer used for collision detection [16]. The gain matrix $\boldsymbol{K}_{\text{reflex}} \in \mathbb{R}^{n\times n}$ is diagonal and positive definite with $K_{\text{reflex},i}$ denoting the i-th diagonal element.

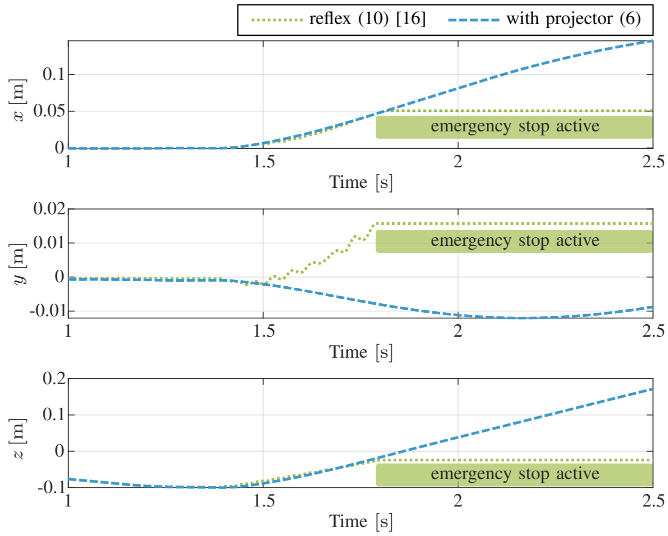

Fig. 6. Experiment 2: Position of the end-effector in x-,y-,z-directions with the reflex strategy (10) [16] (dotted) and the proposed controller (6) (dashed)

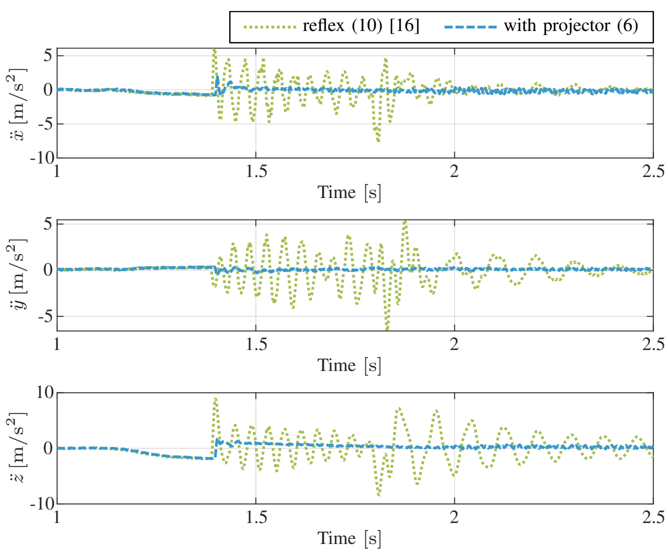

Fig. 7. Experiment 2: Acceleration of the end-effector in x-,y-,z-directions with the reflex strategy (10) [16] (dotted) and the proposed controller (6) (dashed)

In this experiment the manipulator is not at rest at the moment of collision. It moves in z-direction and collides with a paper box (Fig. 1). We deploy the momentum-based observer from [16] to estimate the external torques. If the estimated external torque in one joint exceeds the defined limit $\boldsymbol{\tau}_{\text{limit}} = \left[9, 9, 4, 4, 1.5, 1.5, 1.5\right]^T$ Nm, a collision is detected and the control law is switched from a Cartesian impedance controller [28] to either (10) or (6). We tuned the controller gains such that a comparable motion in z-direction (see bottom plot of Fig. 6) after activation of the reaction controller is achieved. We used $K_{\text{reflex},i} = 4$ for all $i = 1...n$ for the reflex strategy (10) and $\ddot{z}_{\text{des},0} = 5\,\text{m/s}^2$ for the proposed reaction controller (6). Fig. 6 shows that the reflex motion (dotted line) stops abruptly at $t = 1.8\,\text{s}$.

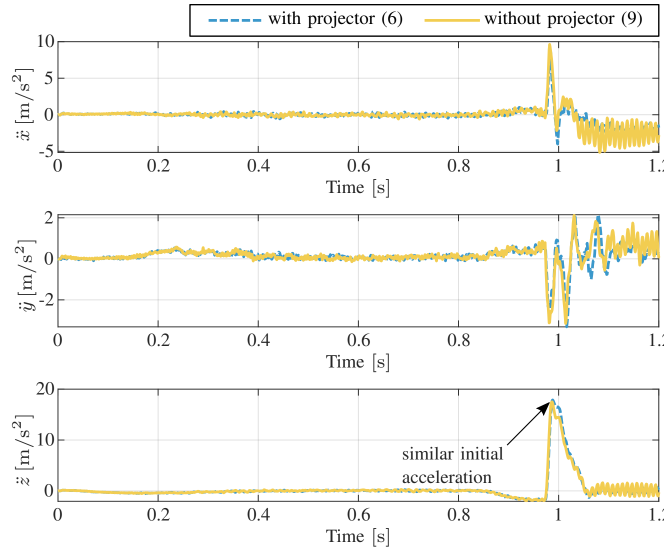

Fig. 8. Experiment 3: Acceleration of the end-effector in x-,y-,z-directions with the proposed strategy with dynamically-consistent null space projector (6) (dashed) and the method without projection (9) (solid) with initial velocity

This is due to pressing the emergency stop, because the system became marginally unstable. This is also illustrated by the oscillations that can be observed in the associated accelerations in x-, y- and z-directions (Fig. 7). Increasing the gains of the reflex controller (10) to $K_{\text{reflex},i} = 5$ for all $i = 1...n$ reinforces this effect and led to instability.

With the oscillations that occurred with the reflex controller (10) it is hard to assess the accelerations for both reaction strategies shown in Fig. 7. The accelerations of the reflex strategy (10) appear much higher, but this high-frequency oscillation in the acceleration signal is only due to the stability margin and cannot be seen in the positions shown in Fig. 6. The deviation of the position in x-direction is comparable in both strategies ((10) and (6)).

The advantages of the theory (6) as seen in Sec. IV are not as clear in the experiments. One recognizes couplings (Fig. 6), which could be reduced by a higher quality of the model. One advantage of the proposed strategy (6) over the reflex strategy (10) is that no problems with marginally stable behavior have been present. In our experimental setup we could not increase the controller gain of the reflex strategy (10) any further due to stability problems. The maximum speed with which we moved away from the collision in the second experiment was $\dot{z}_{\max} = 0.1\,\text{m/s}$. In that regard the proposed reaction control (6) is more robust. This can be due to the fact that the estimated external torque from the observer is not used in the proposed reaction control (6). Since the reflex strategy (10) is directly using the residual $\boldsymbol{r}$ from the momentum-based observer [16], it is more dependent on its dynamics.

The feasible gain for the reflex strategy (10) that we could achieve with our experimental setup, results in rather slow reactive motions. Since the advantage of dynamical decoupling comes into play at faster motions, we conducted

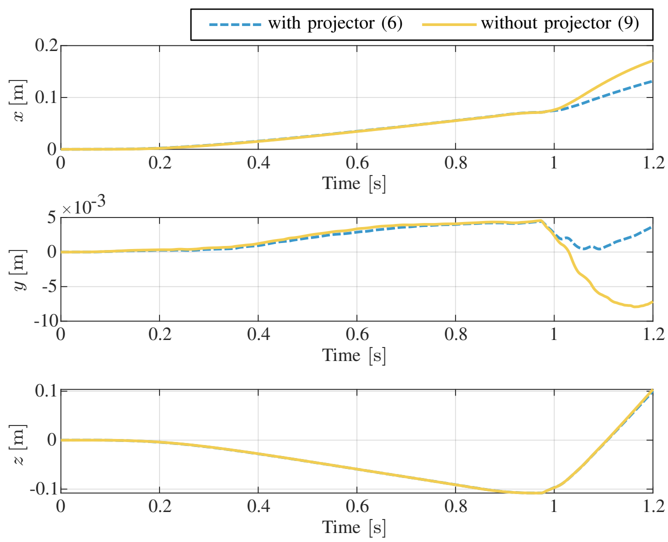

Fig. 9. Experiment 3: Position of the end-effector in x-,y-,z-directions with the proposed strategy with dynamically-consistent null space projector (6) (dashed) and the method without projection (9) (solid) with initial velocity

a third experiment, comparing the proposed strategy (6) and the method without projection (9) in a more dynamic setting. Due to the limitations of the reflex control (10) that we saw in the previous experiment for the given parameters in our experimental setup, a comparison with the reflex strategy (10) is not included at this point.

In the third experiment the end-effector is moving more dynamically in x- and z-directions until it collides. The collision is detected using the momentum-based observer [16]. With $\ddot{z}_{\mathrm{des},0} = 30\,\mathrm{m/s^2}$ for the proposed strategy (6) and $\ddot{z}_{\mathrm{des},0} = 23\,\mathrm{m/s^2}$ for the method without projection (9), we could achieve a maximum acceleration in the desired z-direction of comparable magnitude (see bottom plot of Fig. 8).

The resulting acceleration of the end-effector in x-,y- and z-directions with the proposed strategy with dynamically-consistent null space projector (6) and the method without projection (9) are presented in Fig. 8. One cannot see a significant difference in the accelerations from (6) and (9). The respective position of the end-effector (Fig. 9) shows similar results as in the first experiment (Fig. 5). The end-effector moves about $0.2\,\mathrm{m}$ in the desired z-direction after the collision occurred (see bottom plot of Fig. 9). With the proposed strategy (6) the motion in x- and y-direction is about $0.06\,\mathrm{m}$ and $0.004\,\mathrm{m}$, respectively (dashed line in Fig. 9). With the strategy without projection (9) the deviation is about $0.1\,\mathrm{m}$ in x-direction and $0.007\,\mathrm{m}$ in y (solid line in Fig. 9).

VI. Conclusion

In this work a dynamically-consistent collision reaction control for collaborative robots was presented. It is designed such that the reactive motion is performed in one particular desired direction in task-space (e.g. always away from a human operator). This results in a more predictable behavior for the end-effector motion. Dynamical simulations confirm the theoretical claims and show that the robot is accelerating in the desired direction without disturbing the other ones. The experimental evaluation on a torque controlled KUKA LWR IV+ robot shows the effect of the null space projector. The proposed approach shows a better performance with respect to conventional methods for realizing a single direction reaction motion. However, due to modelling uncertainties and unmodeled friction the full dynamical decoupling could not be achieved to a similar extent as in simulation. The fact that the control law of the proposed reaction strategy is independent of observer dynamics can be important in practice (e.g. in terms of robustness). An in-depth analysis of the robustness properties of the proposed collision reaction control is part of future work.

Acknowledgment

The authors would like to thank Xuwei Wu for the support related to the hardware used for the experiments.

References

[1] S. Haddadin, A. De Luca, and A. Albu-Schäffer, “Robot collisions: A survey on detection, isolation, and identification,” IEEE Transactions on Robotics, vol. 33, no. 6, pp. 1292–1312, 2017.

[2] H. Onda, T. Hasegawa, and T. Matsui, “Collision avoidance for a 6-dof manipulator based on empty space analysis of the 3-d real world,” in IEEE International Workshop on Intelligent Robots and Systems, Towards a New Frontier of Applications, vol. 2, 1990, pp. 583–589.

[3] D. M. Ebert and D. D. Henrich, “Safe human-robot-cooperation: Image-based collision detection for industrial robots,” in IEEE/RSJ International Conference on Intelligent Robots and Systems (IROS), vol. 2. IEEE, 2002, pp. 1826–1831.

[4] X. Fan, R. Simmons-Edler, D. Lee, L. Jackel, R. Howard, and D. Lee, “Aurasense: Robot collision avoidance by full surface proximity detection,” in 2021 IEEE/RSJ International Conference on Intelligent Robots and Systems (IROS). IEEE, 2021, pp. 1763–1770.

[5] G. Hirzinger, A. Albu-Schäffer, M. Hahnle, I. Schaefer, and N. Sporer, “On a new generation of torque controlled light-weight robots,” in 2001 IEEE International Conference on Robotics and Automation (ICRA), vol. 4. IEEE, 2001, pp. 3356–3363.

[6] A. Bicchi, S. L. Rizzini, and G. Tonietti, “Compliant design for intrinsic safety: general issues and preliminary design,” in Proc. IEEE Int. Symp. Intelligent Robots and Systems, Maui, Hawaii, October 2001, pp. 1864–1869.

[7] Y. Yamada, Y. Hirasawa, S. Huang, Y. Umetani, and K. Suita, “Human-robot contact in the safeguarding space,” IEEE/ASME Transactions on Mechatronics, vol. 2, no. 4, pp. 230–236, 1997.

[8] P. Svarny, J. Rozlivek, L. Rustler, M. Sramek, Ö. Deli, M. Zillich, and M. Hoffmann, “Effect of active and passive protective soft skins on collision forces in human–robot collaboration,” Robotics and Computer-Integrated Manufacturing, vol. 78, p. 102363, 2022.

[9] S. Takakura, T. Murakami, and K. Ohnishi, “An approach to collision detection and recovery motion in industrial robot,” in 15th Annual Conference of IEEE Industrial Electronics Society. IEEE, 1989, pp. 421–426.

[10] A. De Luca and R. Mattone, “Sensorless robot collision detection and hybrid force/motion control,” in Proceedings of the 2005 IEEE International Conference on Robotics and Automation (ICRA). IEEE, 2005, pp. 999–1004.

[11] M. Iskandar, O. Eiberger, A. Albu-Schäffer, A. De Luca, and A. Dietrich, “Collision detection, identification, and localization on the dlr sara robot with sensing redundancy,” in 2021 IEEE International Conference on Robotics and Automation (ICRA). IEEE, 2021, pp. 3111–3117.

[12] K. Suita, Y. Yamada, N. Tsuchida, K. Imai, H. Ikeda, and N. Sugimoto, “A failure-to-safety ”kyozon” system with simple contact detection and stop capabilities for safe human-autonomous robot coexistence,” in Proceedings of 1995 IEEE International Conference on Robotics and Automation, vol. 3. IEEE, 1995, pp. 3089–3096.

[13] T. Matsumoto and K. Kosuge, "Collision detection of manipulator based on adaptive control law," in 2001 IEEE/ASME International Conference on Advanced Intelligent Mechatronics. Proceedings, vol. 1. IEEE, 2001, pp. 177–182.

[14] S. Morinaga and K. Kosuge, "Collision detection system for manipulator based on adaptive impedance control law," in 2003 IEEE International Conference on Robotics and Automation, vol. 1. IEEE, 2003, pp. 1080–1085.

[15] J. Heinzmann and A. Zelinsky, "Quantitative safety guarantees for physical human-robot interaction," The International Journal of Robotics Research, vol. 22, no. 7-8, pp. 479–504, 2003.

[16] A. De Luca, A. Albu-Schäffer, S. Haddadin, and G. Hirzinger, "Collision detection and safe reaction with the dlr-iii lightweight manipulator arm," in 2006 IEEE/RSJ International Conference on Intelligent Robots and Systems. IEEE, 2006, pp. 1623–1630.

[17] T. Xu, J. Fan, Q. Fang, J. Zhao, and Y. Zhu, "Robotic arm collision reaction strategies for safe human–robot interaction without torque sensors," Journal of Mechanics in Medicine and Biology, vol. 19, no. 07, p. 1940034, 2019.

[18] A. De Luca and L. Ferrajoli, "Exploiting robot redundancy in collision detection and reaction," in 2008 IEEE/RSJ International Conference on Intelligent Robots and Systems. IEEE, 2008, pp. 3299–3305.

[19] S. Haddadin, A. Albu-Schäffer, A. De Luca, and G. Hirzinger, "Collision detection and reaction: A contribution to safe physical human-robot interaction," in 2008 IEEE/RSJ International Conference on Intelligent Robots and Systems. IEEE, 2008, pp. 3356–3363.

[20] H. Bruyninckx and O. Khatib, "Gauss' principle and the dynamics of redundant and constrained manipulators," in Proceedings 2000 ICRA. Millennium Conference. IEEE International Conference on Robotics and Automation. Symposia Proceedings, vol. 3. IEEE, 2000, pp. 2563–2568.

[21] O. Khatib, "Inertial properties in robotic manipulation: An object-level framework," The International Journal of Robotics Research, vol. 14, no. 1, pp. 19–36, 1995.

[22] R. Murray, Z. Li, S. Sastry, and S. Sastry, A Mathematical Introduction to Robotic Manipulation. Taylor & Francis, 1994.

[23] K. M. Lynch and F. C. Park, Modern robotics. Cambridge University Press, 2017.

[24] B. Paden and R. Panja, "Globally asymptotically stable pd+ controller for robot manipulators," International Journal of Control, vol. 47, no. 6, pp. 1697–1712, 1988.

[25] S. Wolf and M. Iskandar, "Extending a dynamic friction model with nonlinear viscous and thermal dependency for a motor and harmonic drive gear," in 2018 IEEE International Conference on Robotics and Automation (ICRA). IEEE, 2018, pp. 783–790.

[26] M. Iskandar and S. Wolf, "Dynamic friction model with thermal and load dependency: modeling, compensation, and external force estimation," in 2019 International Conference on Robotics and Automation (ICRA). IEEE, 2019, pp. 7367–7373.

[27] L. Le Tien, A. Albu-Schaffer, A. De Luca, and G. Hirzinger, "Friction observer and compensation for control of robots with joint torque measurement," in 2008 IEEE/RSJ International Conference on Intelligent Robots and Systems. IEEE, 2008, pp. 3789–3795.

[28] A. Albu-Schäffer, C. Ott, and G. Hirzinger, "A unified passivity-based control framework for position, torque and impedance control of flexible joint robots," The International Journal of Robotics Research, vol. 26, no. 1, pp. 23–39, 2007.